Previously Documented Basin-localized Extension on Mercury

The most widely distributed extensional landforms on Mercury seen in images from the Mariner 10 and MESSENGER flybys are within the ~1550-km-diameter Caloris basin (Solomon et al., 2008; Murchie et al., 2008). Although Mariner 10 imaged less than half of the basin, basin-concentric and basin-radial troughs interpreted as graben were identified on interior plains deposits inward of the basin rim (Strom et al., 1975; Melosh and McKinnon, 1988; Watters et al., 2005). MESSENGER's first flyby of Mercury confirmed that graben are present throughout the interior of Caloris and revealed that one system of graben, Pantheon Fossae, consists of troughs strongly radial to a point near the center of the basin (Solomon et al., 2008; Murchie et al., 2008; Head et al., 2008; Watters et al., 2009a, b). During its second flyby, MESSENGER imaged another system of basin-radial and basin-concentric graben in the interior plains of the ~700-km-diameter Rembrandt basin (Watters et al., 2009c). Graben were also discovered in two smaller, comparatively young peak-ring basins, Raditladi and Rachmaninoff, both between 250 and 300 km in diameter (Solomon et al., 2008; Watters et al., 2009b; Prockter et al., 2010). Images obtained during the orbital phase of the MESSENGER mission revealed graben within the interior ring of the 230-km-diameter Mozart peak-ring basin (Blair et al., 2012). The extensional stresses that led to graben formation in the Caloris basin have been postulated to be the result of flexural uplift of the interior in response to loading by volcanic plains emplaced exterior to the basin (Melosh and McKinnon, 1988; Kennedy et al., 2008), inward flow of the lower crust in response to horizontal pressure gradients produced by differences in elevation and crustal thickness (Watters et al., 2005; Watters and Nimmo, 2010), or the radial propagation of vertical dikes from a subsurface magma body (Head et al., 2008). These flyby observations suggested that the formation and modification of impact basins has been a key factor in the localization of extensional tectonic activity on Mercury.

Thermal contraction of cooling volcanic units may have played a role in the formation of graben in the basins on Mercury, particular the mid-sized, peak-ring basins. For an initial basin floor geometry with a central deep zone, circumferentially oriented graben such as those found in the Raditladi, Rachmaninoff, and Mozart peak-ring basins can have formed as a result of thermal contraction of interior plains material (Blair et al., 2012). The distribution and complex patterns of graben in the larger Caloris and Rembrandt basins are more difficult to match with thermal stresses alone.

Spatial Distribution of Wrinkle Ridge–Graben Systems

Buried craters and basins that contain wrinkle ridge–graben systems are distributed throughout the northern plains of Mercury (Fig. DR1). To date, these tectonic systems have been found on the volcanic plains that bury 25 impact features, including ghost craters interior to buried basins, ranging in diameter from ~40 to 300 km. This population is in addition to a larger population (~120) of buried basins and craters in the northern plains that have a wide range of diameters but mostly lack evidence of extensional landforms (Fig. DR1). Wrinkle ridge–graben systems associated with buried craters and basins are also seen in other volcanic plains provinces on Mercury. In the volcanic plains exterior to the Caloris basin, seven buried impact structures with wrinkle ridges and graben have been found to date (Fig. DR2). Although the global extent of buried impact features with wrinkle-ridge–graben systems is not yet known, their presence in large volcanic provinces other than the northern plains suggests that the tectonic processes that formed them were not isolated to a few areas on Mercury.

Finite Element Modeling

We used the finite element code Abaqus [www.simulia.com] to develop axisymmetric models of stress and deformation in a volcanically buried, 50-km-diameter impact crater in a partially filled, 200-km-diameter basin (values of model parameters are listed in Table 1). The crater and basin were assumed to have 1 and 4 km of volcanic fill at their respective centers, and the volcanic unit outside the basin was taken to be 1.5 km thick. For simulations of thermal contraction, the youngest cooling unit was assumed to be 0.5 km thick in the basin interior and 0.1 km thick outside the basin. Simulations of global contraction and thermal contraction were modeled to depths of 20 km and 300 km in radius, whereas models that involved lithospheric flexure, including isostatic uplift and lower crustal flow, extended to 200 km depth and 1000 km in radius from the basin center. Side and bottom boundaries were fixed in all models except for simulations of global contraction, for which a horizontal strain equivalent to 1 km of global radial contraction was applied. We considered models in which the elastic strength of the volcanic unit to that of the shallow underlying crust ranged between a factor of 1 and 10, but we found that different ratios influenced only the absolute magnitude of stresses in the volcanic unit and not the predicted style of faulting. In thermal contraction models, stresses were specified at the time when the youngest cooling unit reached background temperature, whereas stresses in uplift models were specified at the time when viscous regions reached a state of relaxation. The choice of thermal conductivity or viscosity did not influence the calculated stress state.

Model results suggest that uplift of the basin in response either to isostatic forces or lower crustal flow can account for a lack of a preferred graben orientations near the basin center but not for circumferentially oriented graben. In addition, such uplift models

cannot explain why graben are confined within basins and do not extend beyond the basin rims, nor why graben generally have greater widths within ghost craters located inside basins. Models of thermal contraction similarly predict graben without a preferred orientation in the centers of craters and basins, but they also predict circumferential graben (radial stress more extensional than circumferential stress) in regions where the youngest cooling unit thins, consistent with observations of such graben orientations at the edges of buried craters and basins. Moreover, thermal contraction models predict that graben should form only where the youngest cooling unit is thick, e.g., within ghost basins where lavas pooled but not outside the basins. This conclusion follows from calculations of thermal strains, which are a factor of 5 greater for thicker cooling units than for thinner units in the models. The formation of wrinkle-ridge rings over buried basin rims is well matched by global contraction models, because horizontal compressive stresses are greatest where the volcanic unit is thinnest and the radial stress component is more compressive than the circumferential stress component at such locations.

Table DR1. Model parameters adopted for this analysis.

Symbol	Description	Value	Units
ρ_f	Density of volcanic fill	3200 [1]	kg m^{-3}
ρ_c	Density of crust	3200	kg m^{-3}
ρ_m	Density of mantle	3400	kg m^{-3}
E	Young's modulus (in all regions unless specified in the text)	10^{11}	Pa
v	Poisson's ratio	0.25	
η_{lc}	Viscosity of lower crust	10^{21}	Pa s
η_a	Viscosity of asthenosphere	10^{20}	Pa s
G	Gravitational acceleration	3.7	m s^{-2}
$T_{i,s}$	Surface temperature	0	°C
ΔT	Background thermal gradient	10	°C km^{-1}
$T_{i,f}$	Elastic blocking temperature of fill	900	°C
κ_f	Thermal conductivity of fill	1.5	W m^{-1} K-^{1}
κ_b	Thermal conductivity of basement	0.5-1.5	W m^{-1} K^{-1}
η_c	Viscosity of compacting basement	10^{20}	Pa s
α_f	Volumetric coefficient of thermal expansion	3×10^{-5}	$°C^{-1}$

REFERENCES CITED

Blair, D.M., Freed, A.M., Byrne, P.K., Klimczak, C, Solomon, S.C., Watters, T.R., Prockter, L.M., Melosh, H.J., and Zuber, M.T., 2012, Thermally induced graben in peak-ring basins and ghost craters on Mercury: Houston, Texas, Lunar and Planetary Institute, Lunar and Planetary Science 43, CD-ROM, abstract 2501.

Freed, A. M., Herring, T., and Bürgmann, R., 2010, Steady-state laboratory flow laws alone fail to explain postseismic observations: Earth and Planetary Science Letters, v. 300, p. 1–10.

Kennedy, P.J., Freed, A.M., and Solomon, S.C., 2008, Mechanisms of faulting in and around Caloris basin, Mercury: Journal of Geophysical Research, v. 113, E08004, doi: 10.1029/2007JE002992.

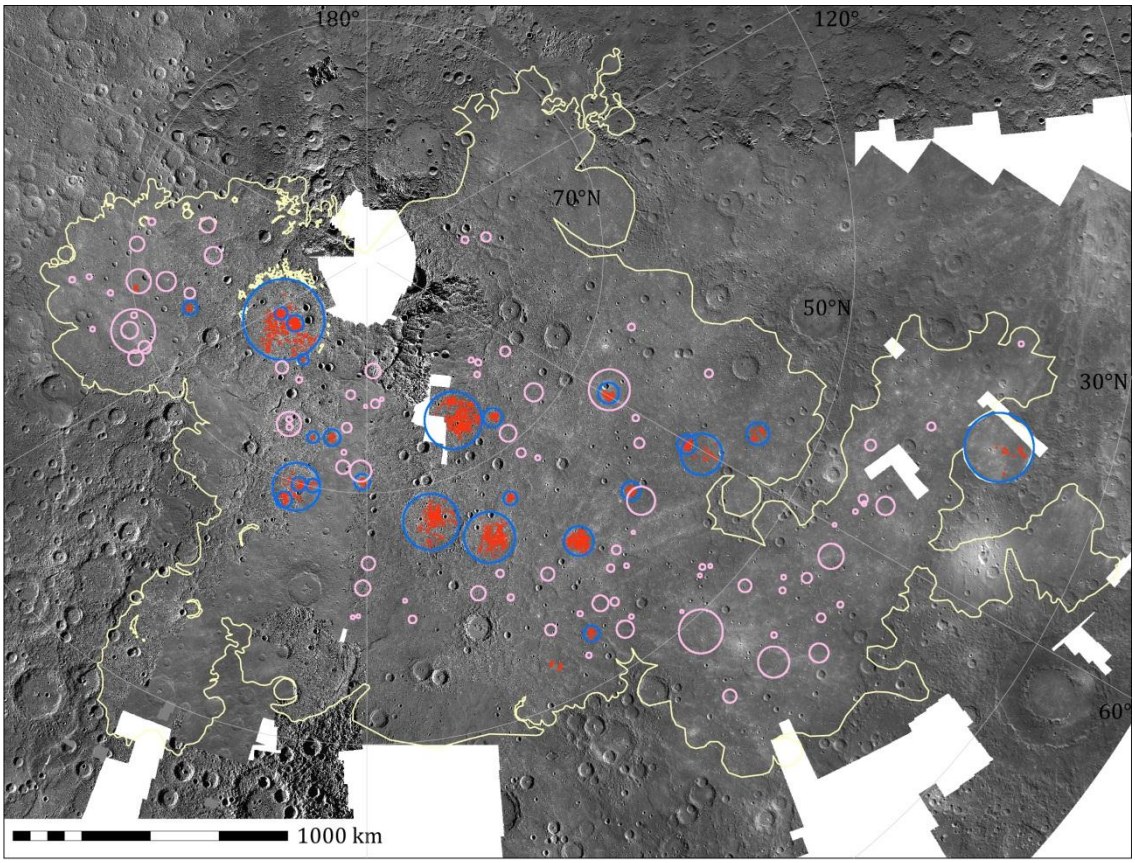

Figure DR1.

Figure DR1. Distribution of buried impact craters and basins delineated by wrinkle-ridge rings in the northern plains. Blue circles mark the locations of buried impact features with wrinkle ridge–graben systems, and pink circles mark the locations of buried impact features that lack graben. The locations of major graben are shown in red. The yellow outline marks the boundary of the northern plains.

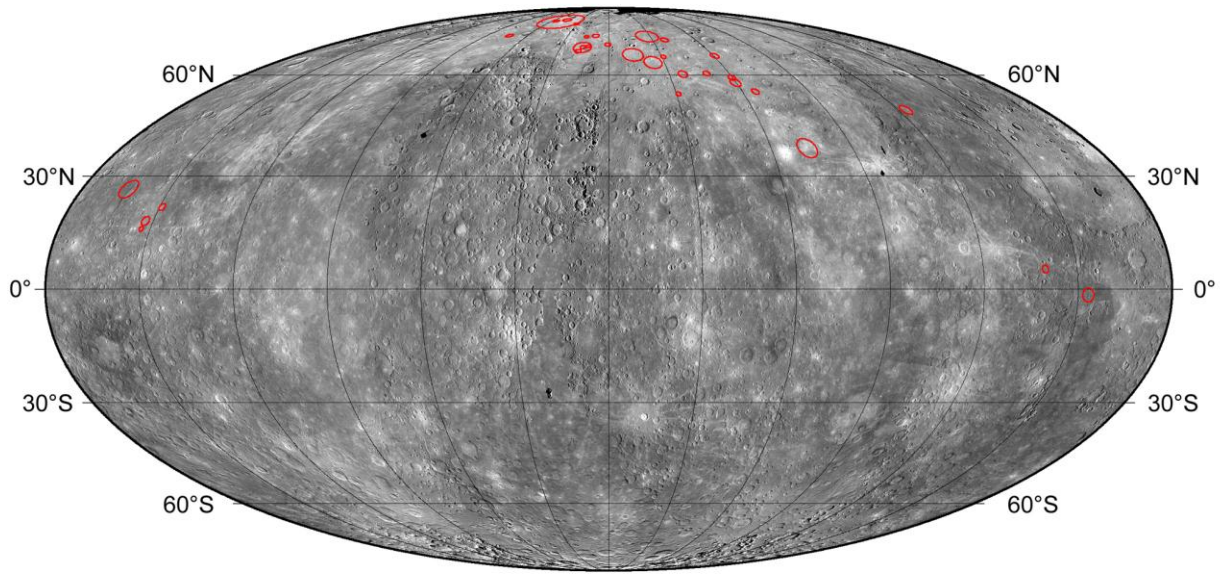

Figure DR2.

Figure DR2. Locations of known occurrences of buried impact features with wrinkle-ridge–graben tectonic systems. Thus far, 32 buried impact craters and basins (red circles) have been documented in the northern plains and in the plains exterior to the Caloris basin. This distribution indicates that wrinkle-ridge–graben systems occur in two of the largest contiguous expanses of volcanic plains material on Mercury. The central longitude of the projection is 180°E.